Journal of Inorganic Biochemistry 193 (2019) 124–129

Contents lists available at ScienceDirect

Journal of Inorganic Biochemistry

journal homepage: www.elsevier.com/locate/jinorgbio

Photochemical property of two Ru(II) compounds based on 5-(2-pyrazinyl) tetrazole for cancer phototherapy by changing auxiliary ligand

Jie Yang[a], Yue Xu[a], Min Jiang[a], Dengfeng Zou[b], Gaowen Yang[a,*], Lei Shen[a,*], Jianhua Zou[a,b,*]

[a] Jiangsu Laboratory of Advanced Functional Material, Department of Chemistry and Material Engineering, Changshu Institute of Technology, Changshu 215500, Jiangsu, PR China

[b] School of Pharmacy, Guilin Medical University, Guilin 541004, Guangxi, PR China

ARTICLE INFO

Keywords:
Ru
Tetrazole
Ligands
PDT
Tumor

ABSTRACT

Ru(II) compounds are potential candidates for photodynamic therapy (PDT) and auxiliary ligands may have an impact on the property of the resulting coordination compounds. In the present study, two Ru(II) compounds based on 5-(2-pyrazinyl)tetrazole (Hpztz) and two classic auxiliary ligands, 2,2′-bipyridine (bipy) or 1,10-phenanthroline (phen) have been prepared and characterized, namely $[Ru(pztz)(bipy)_2][PF_6]$ (**1**) and $[Ru(pztz)(phen)_2][PF_6]$ (**2**). The nanoparticles (NPs) of the two compounds have been prepared by self-assembly in aqueous solution. *In vitro* MTT assay on HeLa cells show that $[Ru(pztz)(phen)_2][PF_6]$ with a lower IC_{50} (half-maximal inhibitory concentration) of only 7.4 μg/mL is superior to that of $[Ru(pztz)(bipy)_2][PF_6]$ (17.8 μg/mL) under irradiation. Meanwhile, negligible dark toxicity have been also observed for the two compounds. In addition, *in vivo* fluorescence imaging suggests that $[Ru(pztz)(phen)_2][PF_6]$ NPs are able to target to the tumor by enhanced permeability and retention effect (EPR). Furthermore, *in vivo* phototherapy on nude mice demonstrate that such NPs can effectively inhibit the growth of the tumor. After treatment for 10 cycles, an obvious decrease in the tumor volume can be observed while the normal tissues, including heart, liver, spleen, lung and kidney, suffer from no damage, indicating the high phototoxicity, low dark toxicity and excellent biocompatibility of $[Ru(pztz)(phen)_2][PF_6]$ NPs.

1. Introduction

Cancer has become the second leading cause of death, following cardiovascular and cerebrovascular diseases, and it has already posed a great threat to the health of human beings. According to the statistics, people in growing number are newly estimated to have been diagnosed with cancer in 2018 [1]. Traditional therapies, such as chemotherapy, radioactive therapy, usually suffer from the disadvantages of invasion, non-targeting and recurrence. Photodynamic therapy (PDT), a relatively newly developed one, is well acknowledged for low systemic toxicity and non-invasion, promising its potential for cancer treatment [2–11]. On the one hand, among the well-established photosensitizers (PSs), for instance, porphyrin (first generation), phthalocyanine (second generation), have been developed as theranostic agents [12–17]. On the other hand, tetrazole-based coordination compounds have been widely used as functional materials, owing to not only their intriguing structure topology, but also potential application as advanced materials, such as magnetism, homogeneous catalysis and energetic materials [18–25]. Ruthenium(II) complexes capable of light-triggered cytotoxicity are appealing potential prodrugs for photodynamic therapy [26–31]. For example, D. Havrylyuk *et.al* reported the photochemical properties and structure-activity relationships of Ru^{II} complexes with pyridylbenzazole ligands as promising anticancer agents [32]. However, investigation concerning Ru(II) compounds based on tetrazole ligands are limited.

Inspired by the observations, to explore the potential of Ru(II) compounds based on tetrazole-carboxylates, two new compounds based on 5-(2-pyrazinyl)tetrazole (Hpztz), namely $[Ru(pztz)(bipy)_2][PF_6]$ (**1**) and $[Ru(pztz)(phen)_2][PF_6]$ (**2**) (phen = 1,10-phenanthroline) have been designed and prepared. The nanoparticles (NPs) of these compounds can be obtained by self-assembly in water. *In vitro* study indicates $[Ru(pztz)(phen)_2][PF_6]$ (**2**) is superior to $[Ru(pztz)(bipy)_2][PF_6]$ (**2**) because the half inhibitory concentration (IC_{50}) of compound **2** is lower than that of compound **1**, which may be ascribed to difference of the auxiliary ligand. Both of the compounds NPs can be uptaken by HeLa cells and capable of generating ROS *in vitro* with DCF as a probe. $[Ru(pztz)(phen)_2][PF_6]$ (**2**) has been chosen to further study the phototherapy efficacy *in vivo*. Fluorescence imaging guided

* Corresponding authors.
E-mail addresses: ygwsx@126.com (G. Yang), leishen@cslg.edu.cn (L. Shen), zoujh93@126.com (J. Zou).

https://doi.org/10.1016/j.jinorgbio.2019.01.015
Received 21 November 2018; Received in revised form 23 January 2019; Accepted 27 January 2019
Available online 28 January 2019
0162-0134/

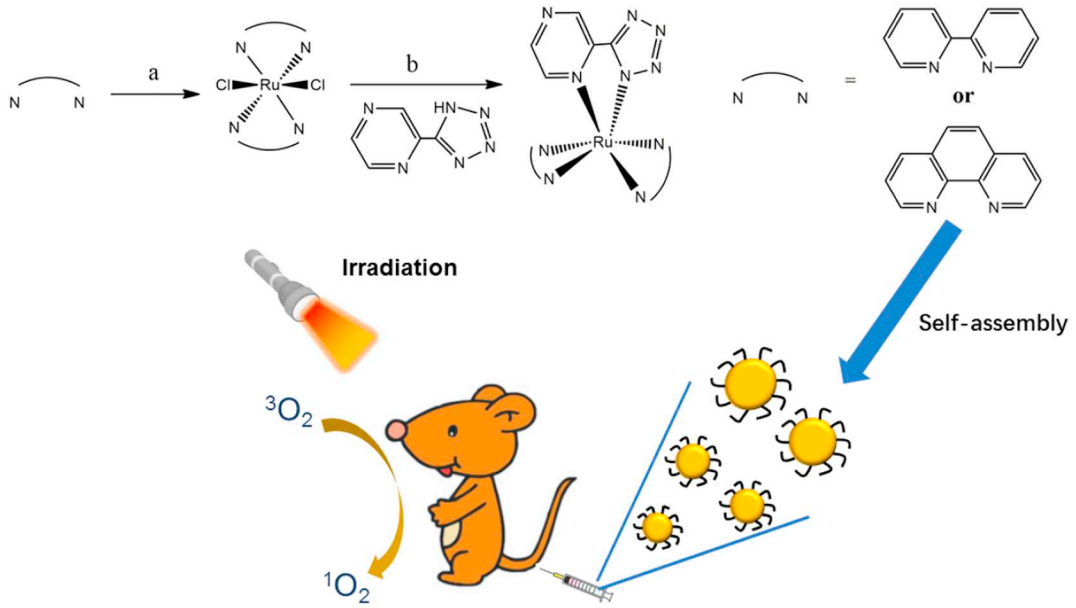

Scheme 1. Illustration of Ru(II) compounds for cancer phototherapy.

phototherapy demonstrate that such NPs can effectively inhibit tumor growth with irradiation while the normal organs suffer from no damage, including heart, liver, spleen, lung and kidney, suggesting the low dark toxicity, high phototoxicity and excellent biosafety of such NPs (see Scheme 1).

2. Experimental section

2.1. Materials and apparatus

All the chemicals were purchased from Sigma (Shanghai Co.Ltd) and used without further purification. The precursors were prepared according to a literature method [33]. The ^{1}H NMR and ^{13}C NMR spectra were recorded on Bruker DRX NMR spectrometer (500 MHz) in DMSO at 298 K as the internal standard (δ = 7.26 ppm). UV-vis spectra were recorded on a spectrophotometer (UV-3600, Shimadzu, Japan). The DLS were measured on a 90 Plus particle size analyzer (Brookhaven Instruments, USA). SEM was conducted on an FEI quanta 200F microscope. The bio-images of the tumor, heart, liver, spleen, and kidney were recorded on a PerkinElmer IVIS Lumina K.

2.2. Synthesis of [Ru(pztz)(bipy)$_2$][PF$_6$] (1)

cis-[RuCl$_2$(bipy)$_2$] (0.52 g, 1 mmol) and NH_4PF_6 (0.539 g, 2.2 mmol) were dissolved in 30 mL ethanol and heated at 90 °C with stirring for 5 h, and the mixture was filtered. Then, a mixture of Hpztz (2 mmol, 0.288 g) and 20 mL ethanol was added to the filtered solution, and the solution was stirred overnight. Next, a mixture of 1 g NH_4PF_6 and distilled water (20 mL) was added to the solution, and the solution was stirred for 10 min. The mixture was extracted with DCM (30 mL) three times and dried with $MgSO_4$. This mixture was then evaporated to dryness under reduced pressure. The crude product was dissolved in some acetone and poured into a large amount of hot ethanol. *Re*-crystallization of the crude product gave rise to the formation of [Ru(pztz)(bipy)$_2$][PF$_6$]. Yield: 40%.^{1}HNMR (500 MHz, DMSO) 9.4 (1H, s), 8.8 (J = 12.8, 7.6, 3.6 Hz, 4H, m), 8.5 (J = 2.4 Hz, 1H, d), 8.1 (J = 20.8, 12.8, 5.2 Hz, 4H, m), 7.9 (J = 5.2 Hz, 1H, d), 7.8 (J = 4.8 Hz, 1H, d), 7.7 (2H, s), 7.6 (J = 17.2, 12.8, 5.6 Hz, 2H, m), 7.5 (2H, s), 7.4 (J = 5.2 Hz,1H, d), ^{13}C NMR (125 MHz, DMSO):160.3, 157.5, 152.2, 146.8, 146.1, 142.7, 138.1, 128.2, 127.5, 124.8, 124.2, 157.16, 152.80, 150.72, 138.84, 137.16, 134.74, 127.35, 125.56, 123.93, 105.44; Elemental analysis: calculated: C: 42.56, H: 2.71, N: 19.85%, found: C: 42.42, H: 2.68, N: 19.81%. MS (ESI) for $C_{25}H_{19}N_{10}RuPF_6$, calculated: 705.52 found: 705.43; IR (KBr, cm^{-1}): 3341(s), 1606(s), 1566(s), 1523(s).

2.3. Synthesis of [Ru(pztz)(phen)$_2$][PF$_6$] (2)

cis-[RuCl$_2$(phen)$_2$] (0.52 g, 1 mmol) and NH_4PF_6 (0.539 g, 2.2 mmol) were dissolved in 30 mL ethanol and heated at 90 °C with stirring for 5 h, and the mixture was filtered. Then, a mixture of Hpztz (2 mmol, 0.288 g) and 20 mL ethanol was added to the filtered solution, and the solution was stirred overnight. Next, a mixture of 1 g NH_4PF_6 and distilled water (20 mL) was added to the solution, and the solution was stirred for 10 min. The mixture was extracted with DCM (30 mL) three times and dried with $MgSO_4$. This mixture was then evaporated to dryness under reduced pressure. The crude product was dissolved in some acetone and poured into a large amount of hot ethanol. *Re*-crystallization of the crude product gave rise to the formation of [Ru(pztz)(phen)$_2$][PF$_6$]. Yield: 35%. ^{1}H NMR (500 MHz, DMSO) 9.42 (J = 17.2, 8.8, 3.6, 4H, m), 8.8 (1H, s), 8.7 (J = 7.2 Hz, 2H, d), 8.4 (2H, s), 8.3 (2H, s), 8.0 (4H, s), 7.6 (J = 8.6 Hz, 3.6 Hz, 4H, t); ^{13}C NMR (125 MHz, DMSO) 160.9, 153.4, 147.8, 145.4, 143.9, 142.6, 130.8, 130.9, 130.1, 128.5, 126.0. Elemental analysis: calculated: C: 46.22, H: 2.54, N: 18.59%, found: C: 46.32, H: 2.58, N: 18.51%. MS (ESI) for $C_{29}H_{19}N_{10}RuPF_6$, calculated: 753.56 found: 753.34; IR (KBr, cm^{-1}): 3341(s), 1606(s), 1566(s), 1523(s).

2.4. Preparation of compound 1 and compound 2 nanoparticles

The nanoparticles of the two compounds were prepared by re-precipitation. Taking compound **1** as an example, 200 μL of [Ru(bipy)$_2$(pztz)](PF$_6$) (10 mg mL^{-1}) in tetrahydrofuran (THF) was added to 5 mL of water under ultrasound at room temperature. After the mixture was stirred for 20 min, THF was removed by purging nitrogen for 20 min.

2.5. Cell culture and MTT assay

HeLa cell lines (Institute of Biochemistry and Cell Biology, SIBS, CAS (China)) were cultured in regular growth medium consisting of Dulbecco's modified Eagle's medium (DMEM, Gibco), supplemented

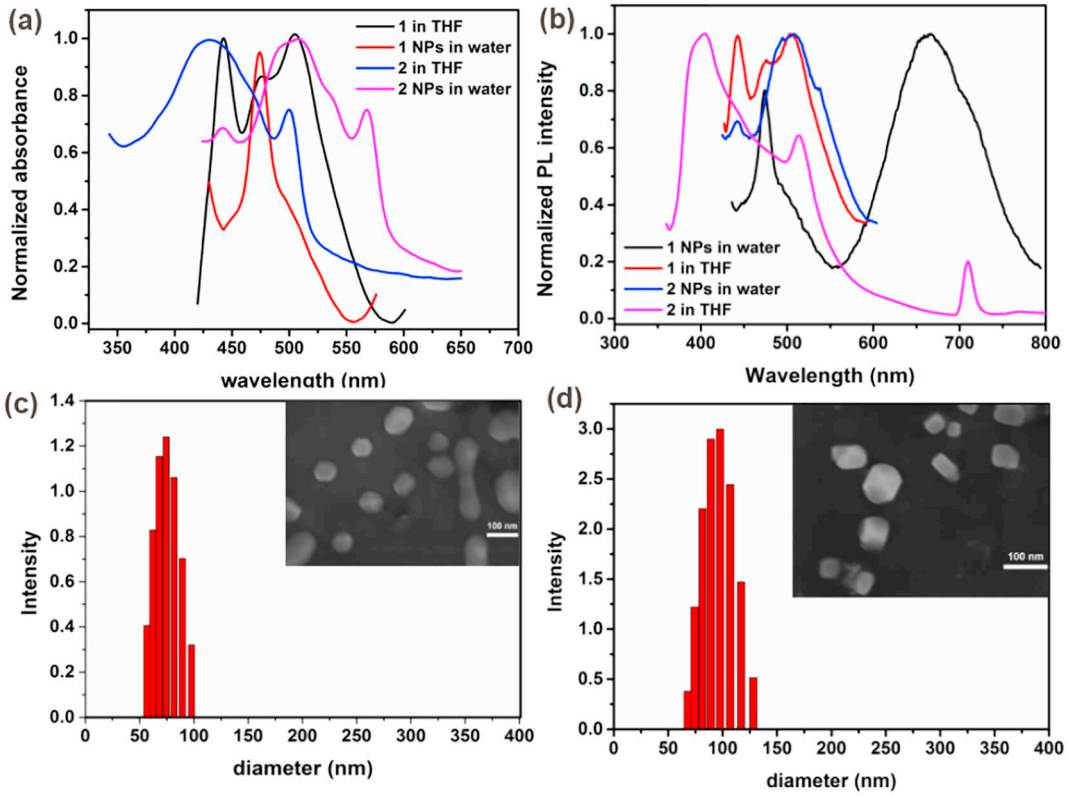

Fig. 1. (a) Normalized absorbance of compounds **1** and **2** in THF and NPs in water; (b) Normalized PL intensity of compounds **1** and **2** in THF and NPs in water; DLS and SEM of NPs of (c) compound **1**; (d) compound **2**.

with 10% fetal bovine serum at 37 °C under a 5% CO_2 atmosphere. Cell viability assays of the nanoparticles of the three compounds were first dissolved in distilled water and then diluted with DMEM to various concentrations and put in the 96-well plate. The incubation time is 24 h. After that, the 96-well plate was irradiated with a xenon lamp (40 mW/cm^2) for 5 min. Cell viability was determined using an MTT (3-(4,5-dimethylthiazol-2-yl)-2,5-diphenyltetrazolium bromide) assay. A solution of MTT in distilled water (5 mg mL^{-1}, 20 mL) was added to each well followed by incubation for 4 h under the same conditions at 37 °C. Then the liquid was discarded and 200 mL DMSO was added. The absorbance at 492 nm of the plate was measured on a Bio-Tek microplate reader at ambient temperature. The cell viability was then determined by the following equation: viability (%) = mean absorbance in each group incubated with different concentrations of NPs/mean absorbance in the control group. The average absorbance of the blank well was subtracted from the readings of the other wells.

2.6. In vitro cellular uptake and fluorescence imaging of cellular ROS

HeLa cells were incubated with the compounds **1** and **2** NPs at the corresponding IC_{50} in a confocal dish for 24 h. Then the solution was discarded and the cells were washed with PBS (3 mL), followed by the addition of 1 mL polyoxymethylene for 25 min. Then polyoxymethylene was discarded and the cells were washed with PBS three times. The sample that was incubated with the compound **1** and **2** NPs for 24 h was further incubated with 10 mM of 2,7-dichlorodihydrofluorescein diacetate (DCF-DA) for another 3 min and was washed with 1 mL PBS three times. This sample was irradiated with a xenon lamp (40 μW cm^{-2}) for 3 min. The fluorescence images were collected using an Olympus IX 70 inverted microscope. The samples incubated with the compound **1** and **2** NPs for 24 h were excited at a wavelength of 405 nm and the fluorescence was collected from 430 to 500 nm. The sample incubated with DCF-DA under irradiation was excited with a 488 nm laser and the fluorescence was collected from 490 to 600 nm.

2.7. In vivo tumor treatment histology examination and bioimaging

The study complies with all institutional and national guidelines and complied with the Chinese laws. Animal ethical approval was obtained from the Guilin Medical University (SCXK2007-001). 12 nude mice were purchased and then injected with HeLa cells as the tumor source into the armpit. When the tumor volumes reached about 100 mm^3, the mice were divided into 3 groups at random. Similarly, the mice in the control group were injected with saline while those in the other two groups were injected with compound **2** NPs. After 24 h, the tumors of the control and illumination groups were irradiated by a Xenon lamp (50 mW/cm^2) for 8 min, whereas the mice in the dark group were not irradiated. The process was conducted for thirty days, and the tumor size and body weight of every mouse were recorded every two days. These nude mice were killed after 30 days, and this was followed by the histology analysis. The main organs (heart, liver, spleen, lung, and kidney) and the tumor from each mouse were isolated and kept in 4% formaldehyde solution. After dehydration, the tissues were embedded in paraffin cassettes and stained with hematoxylin and eosin (H&E), and the images were recorded on a microscope.

3. Results and discussions

3.1. Characterization of $[Ru(pztz)(bipy)_2][PF_6]$ (1) and $[Ru(pztz)(phen)_2][PF_6]$ (2)

The absorbance of compounds $[Ru(pztz)(bipy)_2][PF_6]$ (**1**) and [Ru

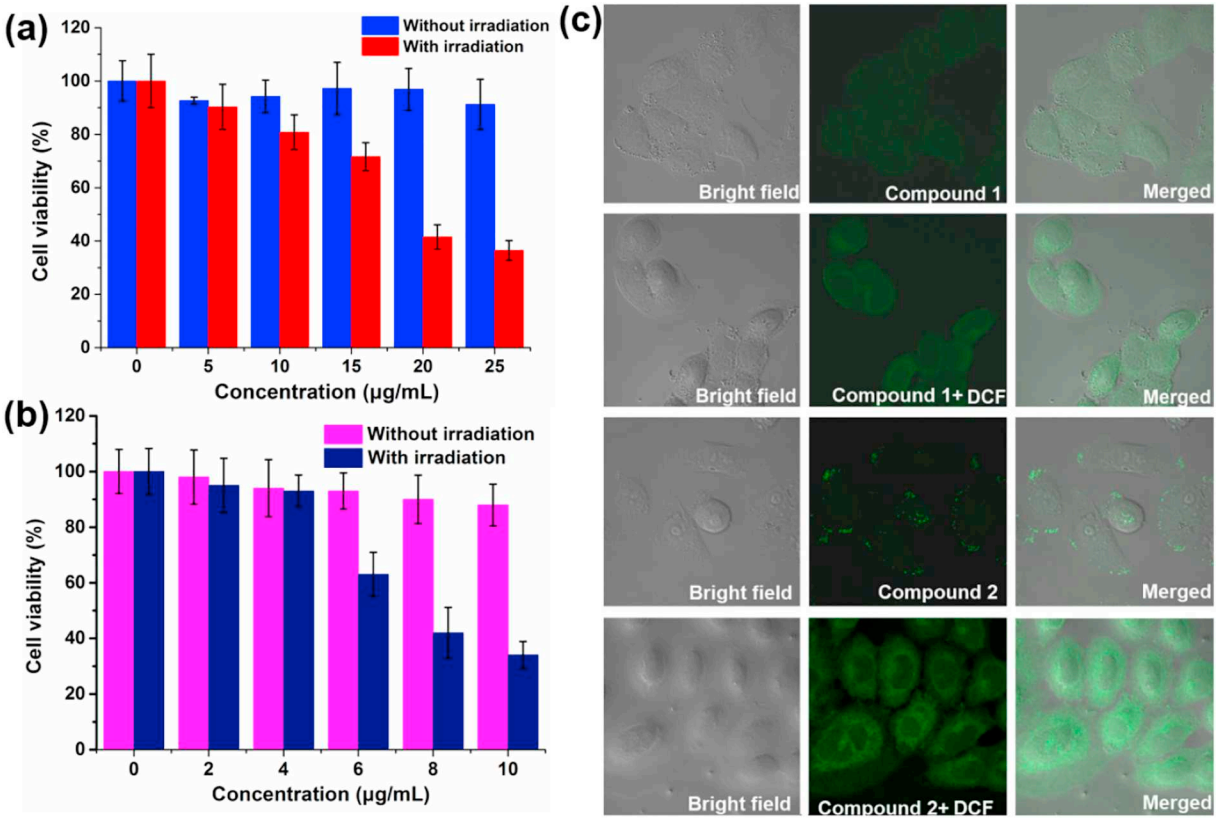

Fig. 2. MTT assay of (a) [Ru(pztz)(2,2′-bipy)$_2$][PF$_6$] (**1**) and [Ru(pztz)(phen)$_2$][PF$_6$] (**2**) NPs; (c) Cellular uptake of compounds **1** and **2** NPs and ROS generation with DCF as probe.

(pztz)(phen)$_2$][PF$_6$] (**2**) in THF and its NPs are shown in Fig. 1a. Compound **1** exhibits two peaks at 432 nm and 508 nm and compound **2** at 422 and 498 nm, respectively. In contrast, the absorbance of NPs in water show red shift. For the emission spectra, red shift was also observed (Fig. 1b). The phenomenon may be attributed to both the aggregation of NPs and the solvent effect. To improve the water dispersity of these compounds, nano-precipitation was used. SEM (scanning electron microscope) and DLS (dynamic light scattering) were used to characterize the size and the diameter of [Ru(pztz)(bipy)$_2$][PF$_6$] (**1**) and [Ru(pztz)(phen)$_2$][PF$_6$] (**2**) NPs. From Fig. 1c and d, it can be seen that the NPs can self-assemble to form hexagon morphology distributing from 52 to 99 nm for compound **1** NPs, and 57 to 128 nm for compound **2** NPs, respectively, suggesting the suitability for enhanced permeability and retention effect (EPR).

3.2. In vitro MTT assay, cellular ROS generation

To explore the PDT efficacy of [Ru(pztz)(bipy)$_2$][PF$_6$] (**1**) and [Ru(pztz)(phen)$_2$][PF$_6$] (**2**) NPs, MTT assay were performed. As shown in Fig. 2a and b, for the irradiation group, cell viability tended to decrease with the increase of the concentration. Both compounds showed high phototoxicity and compound **2** is superior to compound **1** because the IC$_{50}$ (half-maximal inhibitory concentration) of compound **2** (7.4 μg mL^{-1}) is lower than that of compound **1** (17.8 μg mL^{-1}). On the other hand, the cell viability remained high without irradiation, suggesting the low dark toxicity of the compound. Fig. 2c shows the cellular uptake and ROS generation with DCF as a probe of compounds **1** and **2** in HeLa cells. These NPs can be uptaken by HeLa cells as indicated by the green fluorescence. In addition, ROS (reactive oxygen species) can also be generated upon irradiation at 488 nm because the fluorescence can be lighted.

3.3. In vivo fluorescence imaging guided photodynamic therapy

Nanoparticles can be passively targeted to the tumor by EPR effect. Confocal laser scanning microscope (CLSM) has been taken advantage of to investigate the uptake of the NPs in the tumor. As shown in Fig. 3a, no detectable fluorescence can be observed at 0 h. After post-injection for 2 h, the fluorescence of the tumor gradually become stronger while that is the strongest at 6 h injection, indicating 6 h is the appropriate time for phototherapy. At 24 h, the tumor still remain fluorescent. Then the mouse was sacrificed and the fluorescence intensity of the tumor and other five normal tissues, including heart, liver, spleen, lung and kidney were measured. The fluorescence intensity of the tumor is the strongest, followed by liver and kidney, showing the low term retention of such NPs (Fig. 3b).

3.4. In vivo photodynamic therapy

Since the phototherapy efficacy of [Ru(pztz)(phen)$_2$][PF$_6$] is superior to that of [Ru(pztz)(bipy)$_2$][PF$_6$]. In order to evaluate the phototherapy efficacy of [Ru(pztz)(phen)$_2$][PF$_6$] NPs, 12 HeLa tumor-bearing nude mice were divided into three groups at random and used to investigate the PDT efficacy of [Ru(pztz)(phen)$_2$][PF$_6$] NPs *in vivo*. As shown in Fig. 4a, the tumor volume increases quickly while that of the NPs only increase a little slowly. The tumor volume of the control and the no illumination groups jump at a considerable high speed, respectively while that of the illumination group is almost unchanged, indicating the outstanding phototherapy efficacy of [Ru(pztz)(phen)$_2$][PF$_6$] NPs under irradiation. However, the tumor volume of the no illumination group is a little smaller than that of the control group, which can be explained by the fact that the sunlight inevitably irradiate the tumor to inhibit the tumor growth. The body weight in the three groups increase, respectively, indicating the low dark toxicity and good bio-

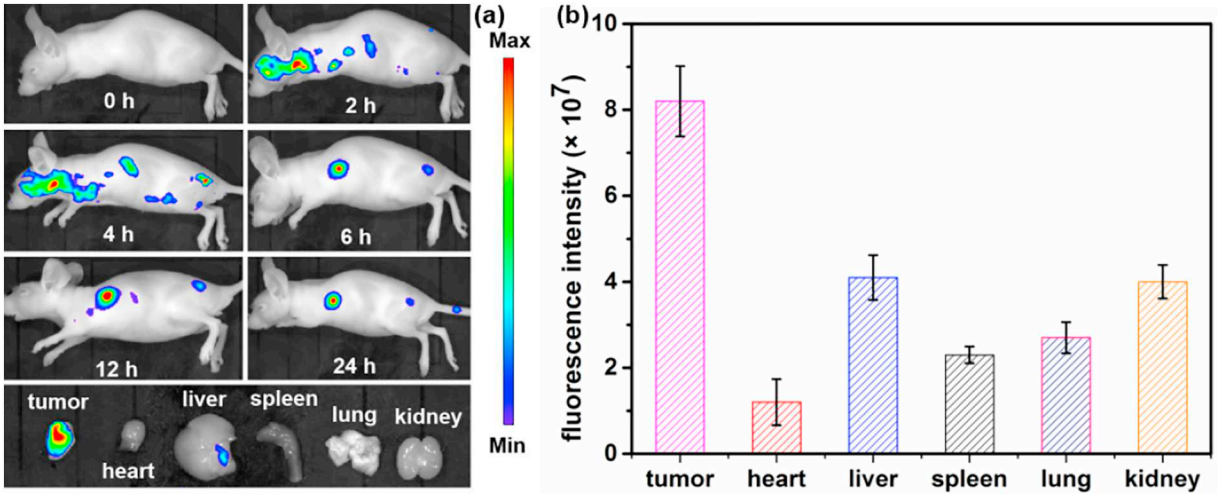

Fig. 3. (a) Fluorescence imaging of $[Ru(pztz)(phen)_2][PF_6]$ NPs in HeLa tumor bearing nude mouse at different period of time (0, 2, 6, 12 and 24 h); (b) Fluorescence intensity of tumor, heart, liver, spleen, lung and kidney of the sacrificed mouse after 24 h intravenous injection.

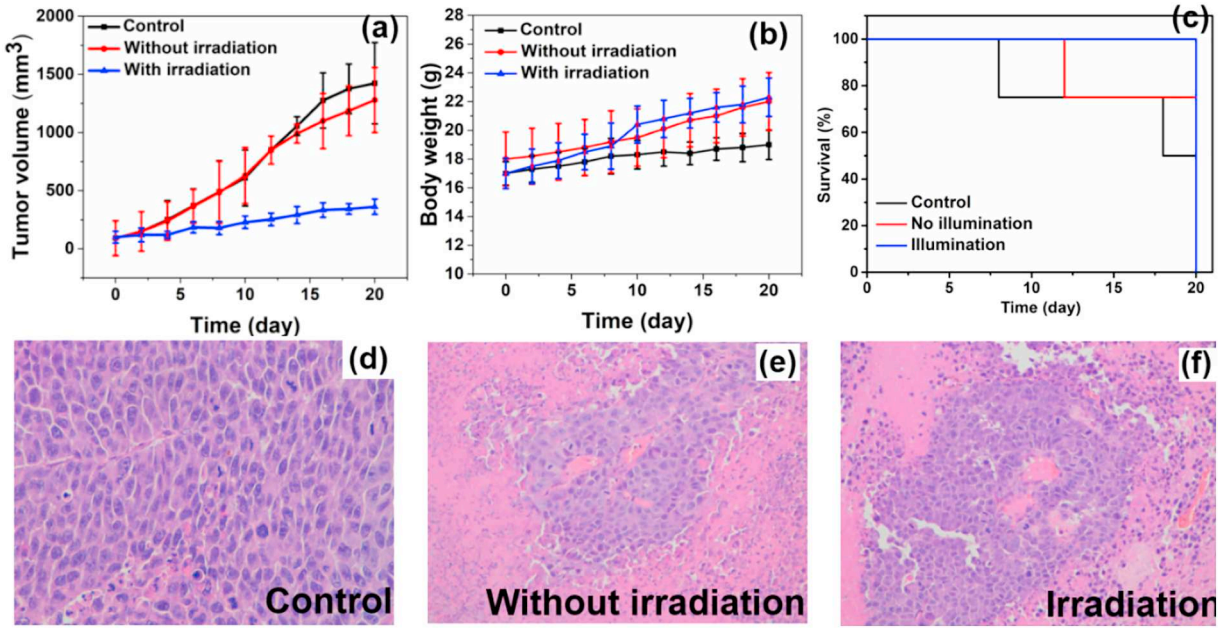

Fig. 4. (a) Tumor volume change of the three groups; (b) Body weight change of the groups; (c) Survival rate in the three groups; (d-f) H&E stained pictures of the tumors in control, without irradiation and irradiation groups.

compatibility of $[Ru(pztz)(phen)_2][PF_6]$ NPs (Fig. 4b). The survival rate of the mice after sacrifice are shown in Fig. 4c. Hematoxylin and eosin (H&E)-stained images of the tumors in the control and no illumination groups (Fig. 4d–f) show the nucleus of HeLa cells remain normal, suggesting the low dark toxicity themselves. In contrast, the nucleus of the irradiation group are distorted or even damaged, indicating the good phototherapy efficacy of $[Ru(pztz)(phen)_2][PF_6]$ NPs.

To further investigate the bio-compatibility of NPs, the H&E stained pictures of the normal organs have been illustrated in Fig. 5. the normal organs (heart, liver, spleen, lung, kidney) in no illumination and illumination groups suffer from no damage, indicating the good biosafety of $[Ru(pztz)(phen)_2][PF_6]$ NPs [30–32].

4. Conclusions

In conclusion, two new Ru(II) compounds based on Hpztz have been prepared by changing the auxiliary ligand, from bipy to phen. The two compounds show both mononuclear structure and the NPs were obtained by self-assembly in water. In addition, negligible dark toxicity was observed while $[Ru(pztz)(phen)_2][PF_6]$ is superior to $[Ru(pztz)(bipy)_2][PF_6]$ in terms of cytotoxicity upon irradiation. Furthermore, both *in vitro* and *in vivo* study show that $[Ru(pztz)(phen)_2][PF_6]$ with a low IC_{50} on HeLa cells can effectively inhibit the growth of tumor and cause no damage to the normal tissues, including heart, liver, spleen, lung and kidney. Our results suggest that $[Ru(pztz)(phen)_2][PF_6]$ with negligible dark toxicity, excellent photo toxicity as well as outstanding biocompatibility may have potential for imaging guided photodynamic therapy.

Conflict of interest

The authors have no conflicts of interest to declare.

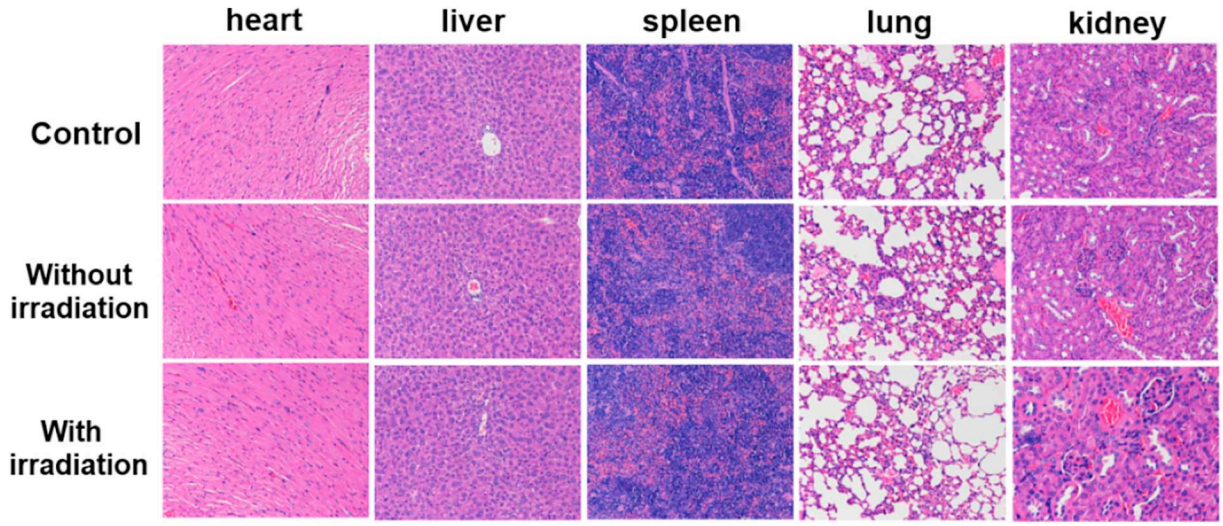

Fig. 5. H&E stained picture of normal organs, including heart, liver, spleen, lung and kidney.

Acknowledgment

The authors acknowledge financial support from the Natural Science Foundation of China (Grant. No. 81460119), National Natural Science Fundation of Jiangsu Province (Grant No. BK2012210), the Natural Science Foundation of the Jiangsu Higher Education Institutions of China (Grant No. 10KJB430001) and the Opening Fund of Jiangsu Key Laboratory of Advanced Functional Materials (Grant No. 12KFJJ010).

References

[1] R.L. Siegel, K.D. Miller, A.J. DVM, CA Cancer J. Clin. 68 (2018) 7–30.
[2] W.P. Fan, P. Huang, X.Y. Chen, Chem. Soc. Rev. 45 (2016) 6488–6519.
[3] Z.J. Zhou, J.B. Song, L.M. Nie, X.Y. Chen, Chem. Soc. Rev. 45 (2016) 6597–6626.
[4] Z.F. Chang, L.M. Jing, B. Chen, M.S. Zhang, X.L. Cai, J.J. Liu, Y.C. Ye, X.D. Lou, Z.J. Zhao, B. Liu, J.L. Wang, B.Z. Tang, Chem. Sci. 7 (2016) 4527–4536.
[5] X. Liu, M. Wu, Q. Hu, H. Bai, S. Zhang, Y. Shen, G. Tang, Y. Ping, ACS Nano 10 (2016) 11385–11396.
[6] E. Palao, T. Slanina, L. Muchova, T. Solomek, L. Vitek, P. Klan, J. Am. Chem. Soc. 138 (2016) 126–133.
[7] S.H. Wang, L. Shang, L.L. Li, Y.J. Yu, C.W. Chi, K. Wang, J. Zhang, R. Shi, H.Y. Shen, G.I.N. Waterhouse, S.J. Liu, J. Tian, T.R. Zhang, H.Y. Liu, Adv. Mater. 28 (2016) 8379–8387.
[8] M. Li, Y. Gao, Y.Y. Yuan, Z. Wu, Z.F. Song, B.Z. Tang, B. Liu, Q.C. Zheng, ACS Nano 11 (2017) 3922–3932.
[9] J. Yang, X.Q. Gu, W.T. Su, X.Y. Hao, Y.J. Shi, L.Y. Zhao, D.F. Zou, G.W. Yang, Q.Y. Li, J.H. Zou, Mater. Chem. Front. 2 (2018) 1842–1846.
[10] W. Sun, M. Parowatkin, W. Steffen, H.J. Butt, V. Mailänder, S. Wu, Adv. Healthc. Mater. 5 (2016) 467–473.
[11] S.C. Boca, M. Four, A. Bonne, B. van der Sanden, S. Astilean, P.L. Baldeck, G. Lemercier, Chem. Commun. (2009) 4590–4592.
[12] D.P. Ferreir, D.S. Conceicão, R.C. Calhelha, T. Sousa, I.C.F.R. Radu Socoteanu, L.F. Ferreira, Vieira Ferreira, Carbohydr. Polym. 251 (2016) 167–171.
[13] C. Conte, A. Scala, G. Siracusano, G. Sortino, R. Pennisi, A. Piperno, A. Miroa, F. Ungaroa, M.T. Sciortino, F. Quagliaa, A. Mazzaglia, Colloids Surf. B: Biointerfaces 146 (2016) 590–597.
[14] M. Göksel, Bioorg. Med. Chem. 24 (2016) 4152–4164.
[15] Z. Yang, W.P. Fan, W. Tang, Z.Y. Shen, Y.L. Dai, J.B. Song, Z.T. Wang, Y. Liu, L.S. Lin, L.L. Shan, Y.J. Liu, O. Jacobson, P.F. Rong, W. Wang, X.Y. Chen, Angew. Chem. Int. Ed. 57 (2018) 14101–14105.
[16] S.H. Wang, L. Shang, L.L. Li, Y.J. Yu, C.W. Chi, K. Wang, J. Zhang, R. Shi, H.Y. Shen, G.I.N. Waterhouse, S.J. Liu, J. Tian, T.R. Zhang, H.Y. Liu, Adv. Mater. 28 (2016) 8379–8387.
[17] J.F. Zhou, L.Z. Gai, Z.K. Zhou, W. Yang, J. Mack, K.J. Xu, J.Z. Zhao, Y. Zhao, H.L. Qiu, K.S. Chan, Z. Shen, Chem. Eur. J. 22 (2016) 13201–13209.
[18] G. Aromi, L.A. Barrios, O. Roubeau, P. Gamez, Coord. Chem. Rev. 255 (2011) 485–546.
[19] Q.Y. Li, D.Y. Chen, M.H. He, G.W. Yang, L. Shen, C. Zhai, W. Shen, K. Gu, J.J. Zhao, J. Solid State Chem. 190 (2012) 196–201.
[20] D.Y. Chen, J.H. Zou, W.X. Li, B. Xu, Q.Y. Li, G.W. Yang, J. Wang, Y.M. Ding, Y. Zhang, X.F. Shen, Inorg. Chem. Commun. 40 (2014) 35–38.
[21] G.W. Yang, D.Y. Chen, C. Zhai, X.Y. Tang, Q.Y. Li, F. Zhou, Z.F. Miao, J.N. Jin, H.D. Ding, Inorg. Chem. Commun. 14 (2011) 913–915.
[22] Y.M. Lu, J. Wang, J. Wu, K.K. Ding, Y.K. Li, L.L. Miao, Q.Y. Li, G.W. Yang, Inorg. Chim. Acta 450 (2016) 395–401.
[23] C. Zhai, Z.Y. Yang, D. Xu, Z.K. Wang, X.Y. Hao, Y.J. Shi, G.W. Yang, Q.Y. Li, J. Solid State Chem. 258 (2018) 156–162.
[24] C. Zhai, L. Zhao, X.Y. Hao, Y.J. Shi, D. Xu, Z.Y. Yang, Z.K. Wang, D.Y. Chen, Q.Y. Li, G.W. Yang, Inorg. Chem. Commun. 84 (2017) 150–152.
[25] J.H. Zou, D.Y. Chen, G.W. Yang, Q.Y. Li, J. Yang, L. Shen, RSC Adv. 5 (2015) 27887–27890.
[26] R. Arakawa, S. Mimura, G. Matsubayashi, T. Matsuo, Photolysis, Inorg. Chem. 35 (1996) 5729.
[27] W. Sun, R. Thiramanas, L.D. Slep, X.L. Zeng, V. Mail-nder, S. Wu, Chem. Eur. J. 23 (2017) 10832–10837.
[28] W. Sun, S.Y. Li, B. Häupler, J. Liu, S.B. Jin, W. Steffen, U.S. Schubert, H.J. Butt, X.J. Liang, S. Wu, Adv. Mater. 29 (2017) 1603702.
[29] K. Fujita, Y.Y. Tanaka, T. Sho, S.C. Ozeki, S. Abe, T. Hikage, T. Kuchimaru, S.K. Kondoh, Ta. Ueno, J. Am. Chem. Soc. 136 (2014) 16902–16908.
[30] G.W. Yang, X. Zhang, G.M. Li, J. Yang, L. Shen, D.Y. Chen, Q.Y. Li, D.F. Zou, New J. Chem. 42 (2018) 5395–5402.
[31] B. Wei, M.Y. Guo, Y.M. Lu, P.P. Sun, G.W. Yang, Q.Y. Li, Z. Anorg. Allg. Chem. 644 (2018) 6–11.
[32] D. Havrylyuk, D.K. Heidary, L. Nease, S. Parkin, E.C. Glazer, Eur. J. Inorg. Chem. (2017) 1687–1694.
[33] R. Arakawa, S. Mimura, G. Matsubayashi, T. Matsuo, Inorg. Chem. 35 (1996) 5729.